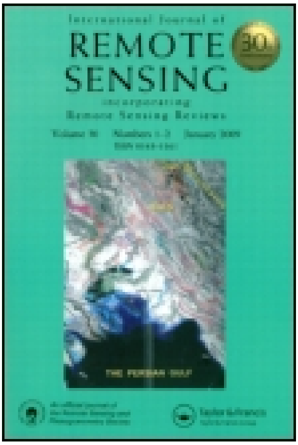

International Journal of Remote Sensing
Publication details, including instructions for authors and subscription information:
http://www.tandfonline.com/loi/tres20

SPOT VEGETATION for characterizing boreal forest fires

R.H. Fraser [a] , Z. Li [b] & R. Landry [b]
[a] Intermap Technologies, Canada Centre for Remote Sensing, Ottawa, Ontario
[b] Canada Centre for Remote Sensing, Ottawa, Ontario, Canada

Available online: 25 Nov 2010

INT. J. REMOTE SENSING, 2000, VOL. 21, NO. 18, 3525–3532

SPOT VEGETATION for characterizing boreal forest fires

R.H. FRASER

Intermap Technologies, Canada Centre for Remote Sensing, Ottawa, Ontario, Canada; e-mail: robert.fraser@ccrs.nrcan.gc.ca

Z. LI and R. LANDRY

Canada Centre for Remote Sensing, Ottawa, Ontario, Canada

(*Received 16 November 1999; in final form 16 March*)

Abstract. The potential of the recent SPOT VEGETATION (VGT) sensor for characterizing boreal forest fires was investigated. Its capability for hotspot detection and burned area mapping was assessed by analysing a series of VGT, NOAA/AVHRR, and Landsat TM images over a 1541 km^2 fire that occurred in May 1998, in Alberta, Canada. VGT's 1.65 μm, short-wave infrared (SWIR) channel was capable of detecting thermal emissions from intense fires, although it was considerably less sensitive to hotspots than the 3.7 μm channel from NOAA's Advanced Very High Resolution Radiometer (AVHRR). The SWIR also enabled burned areas to be more easily discriminated compared to the visible and near-infrared (NIR) channels. The SWIR and NIR channels were combined to produce a new index that provides better separation of burned forest with less sensitivity to smoke aerosol than the commonly used Normalized Difference Vegetation Index (NDVI).

1. Introduction

The boreal forest zone, composed primarily of conifer trees north of 45°, covers an area of 12 million km^2 and accounts for 25% of the world's forests. This zone is subject to large, intense fires that burn an average 2.4 million ha annually in Canada (Stocks 1991) and as much as 22 million ha globally in a single year (Cofer *et al.* 1996). Wildfires are a dominant influence on the boreal biome, controlling successional patterns, primary productivity, and carbon cycling (French *et al.* 1996). Boreal fires also inject large amounts of trace gases and smoke aerosol into the atmosphere, both of which influence the Earth's radiation budget (Levine *et al.* 1995). Considering the remoteness and vast extent of the boreal biome, satellite remote sensing is particularly well suited to documenting the spatial and temporal distribution of fires so that these impacts may be quantified.

Analysis of boreal fires using satellite sensors has relied primarily on NOAA's AVHRR, providing daily coverage at a coarse 1.1-km spatial resolution. Burned areas have been successfully mapped in Alaska (Kasischke and French 1995) and Canada (Fraser *et al.* 2000, Li *et al.* 2000a) through multi-temporal analysis of the NDVI. Cahoon *et al.* (1994) used unsupervised minimum distance classification to identify 14 million ha of east-Asian boreal forest that burned in 1987. Active boreal fires have also been detected using AVHRR by exploiting the high sensitivity of the

International Journal of Remote Sensing
ISSN 0143-1161 print/ISSN 1366-5901 online © 2000 Taylor & Francis Ltd
http://www.tandf.co.uk/journals

3.7 μm channel to targets with thermal emissions in the range for vegetation fires (Flannigan and Vonder Haar 1986, Rauste *et al.* 1997, Li *et al.* 2000b).

The SPOT VEGETATION (VGT) sensor, launched in 1998, has a swath and resolution that is comparable to AVHRR, but possesses spectral bands specifically tailored for large-area vegetation monitoring, i.e. 0.43–0.47 μm (blue), 0.61–0.68 μm (red), 0.78–0.89 μm (NIR), and 1.58–1.75 μm (SWIR). The purpose of the present Letter is to describe the potential of VGT imagery for detecting boreal forest fires and identifying burned areas. A massive forest fire that occurred during May 1998 in Alberta, Canada served as a case study.

2. Study area

The Virginia Hills are situated about 200 km northwest of Edmonton, Alberta, at approximately 55° N and 116° W. The study area, lying within the Lower Foothill of the Boreal Forest Region, comprises hardwood, softwood, and mixedwood stands, clear-cuts, regeneration, numerous regenerating burns, wetlands, small lakes, and seismic survey lines (Kneppeck and Ahern 1989). Tree species include white spruce (*Picea glauca*), black spruce (*Picea mariana*), lodgepole pine (*Pinus contorta*), balsam fir (*Abies balsamea*), balsam poplar (*Populus balsamifera*), and trembling aspen (*Populus tremuloides*).

A fire was detected in the area on 3 May 1998, which spread rapidly due to extreme fire weather conditions. The official estimate of the area damaged is 1541 km^2 (154 094 ha), the majority of which burned between 4–5 May before dying out in late May. Although fires of this magnitude are infrequent in Canada, fires larger than 100 000 ha were responsible for 26% of the forest area burned between 1990–1995 (Canadian Council of Forest Ministers 1999).

3. Satellite sensor data

As a participant in the SPOT VEGETATION Preparatory Programme, we obtained single SPOT VGT scenes (P products) covering Central Canada for selected passes between 30 April–31 June and all passes between 1 July–31 August 1998. The imagery consisted of calibrated, top-of-atmosphere (TOA) reflectance for four channels, registered by bi-cubic interpolation to zone 12 of the Universal Transverse Mercator (UTM) co-ordinate system. Since geo-location for these early VGT images relied on satellite orbit and attitude, registration was manually fined tuned to within one pixel using small lakes in the area surrounding the fire. From the VGT database, one pre-fire (2 May), two active fire (5 May, 8 May), and 10 post-fire (10 May–30 August) scenes were selected providing cloud-free coverage of the area affected by burning. A NOAA-14/AVHRR image acquired 5 May was calibrated and precision geocoded (Li *et al.* 2000b) to compare VGT's fire detection capability with that of AVHRR.

Cloud-free Landsat TM scenes providing coverage of the study area were acquired for 30 April 1998, 10 June 1998, and 30 August 1998. False colour TM composites were used to interpret pre-fire vegetation types and delineate training regions in the VGT imagery. Figure 1(*a*) shows a 10 June false-colour TM composite (SWIR,NIR,Red = RGB), in which the Virginia Hills burn appears dark red, recent clear-cuts are pink, hardwood aspen stands are light green, and softwood coniferous forest is dark green (Ahern and Archibald 1986). A VGT composite from the same

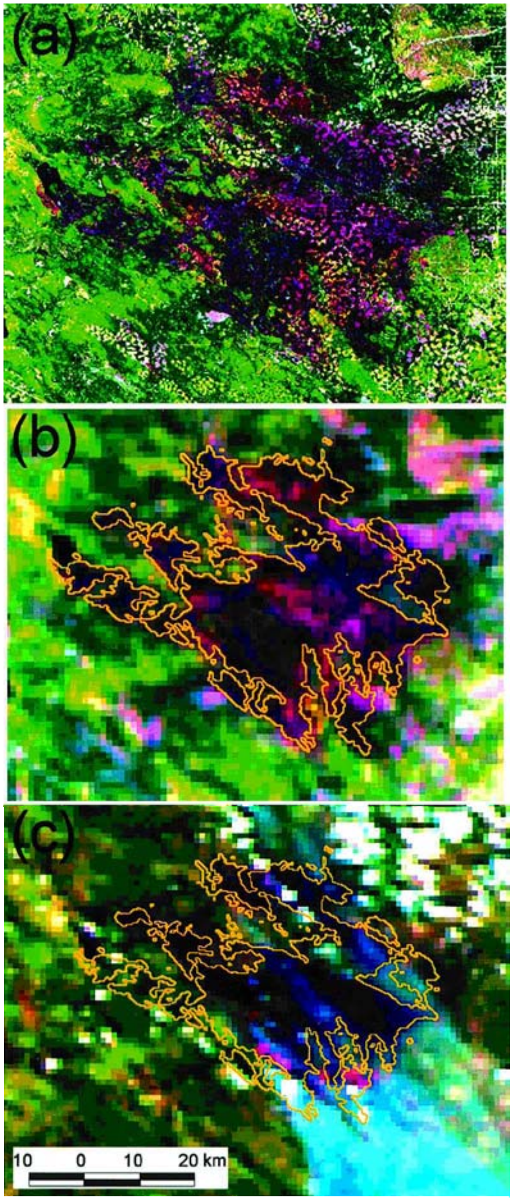

Figure 1. The Virginia Hills burn as imaged on 10 June, 1998 by (*a*) Landsat TM (5,4,3 = RGB) and (*b*) SPOT VEGETATION (4,3,2 = RGB). Burned areas appear red due to the large relative reflectance in the SWIR channel. (*c*) Active fires appear red in a VEGETATION composite (4,3,2 = RGB) acquired on 5 May, 1998 due to thermal emissions in the SWIR. Burned areas initially exhibit decreased reflectance in all channels, thus appearing black. Smoke plumes (blue) are visually separable from cloud (white) due to low reflectance in the SWIR. The outer burn perimeter as derived from TM interpretation is overlaid in (*b*) and (*c*).

date displayed using analogous channels (figure 1(*b*)) appears as a blurred version of the TM image and similarly provides excellent discrimination of burned forest and other general cover types.

4. Active fire detection

According to Plank's equation, a flaming boreal fire at 1000 °K has a blackbody spectral exitance of 3590 $Wm^{-2} \mu m^{-1}$ at the centre of AVHRR's 3.7 μm channel. VGT's SWIR channel at 1.65 μm would receive only 1590 $Wm^{-2} \mu m^{-1}$ from such a fire. This weaker response, combined with an earlier overpass time (late-morning vs. mid-afternoon for NOAA-14/AVHRR) when boreal fires are less active, makes VGT sub-optimal for fire detection. Nevertheless, several hotspot pixels are evident in the fire front on 5 May and 8 May VGT images acquired during the Virginia Hills fire (e.g. figure 1(*c*)), as well as in images containing other 1998 boreal fires. We noted, however, that significantly more hotspots are observable in the 3.7 μm channel from the AVHRR image obtained during the fire. An AVHRR fire detection algorithm (Li *et al.* 2000b) detects 295 hotspot pixels over the fire from the 5 May NOAA-14/AVHRR image, while only approximately 40 pixels are observed to have a significantly elevated SWIR signal in the 5 May VGT image (figure 1(*c*)). The SWIR channel, unlike AVHRR, was rarely saturated by fire and thus could be used to provide a measure of boreal fire size/intensity.

5. Spectral signature of burned forest

To investigate VGT spectral response to burning, several polygons were manually delineated on the VGT imagery representing burned softwood forest (80 pixels) and undisturbed softwood forest (84 pixels) surrounding the burned area. The pre-fire VGT and TM scenes aided in selecting unburned forest that had similar species composition to the burned forest polygons prior to burning. A cloud mask was applied to each VGT scene ($ch2_{TOA} > 0.2$) to remove any cloud-contaminated pixels from consideration before calculating reflectance statistics. The temporal evolution of TOA reflectances, shown using the ratio of burned to non-burned reflectance, is presented in figure 2 (a ratio is used to minimize atmospheric and BRDF variations). Sampling dates cover the period from 2 May, one day before the fire was detected, until 30 August, 121 days later.

The blue channel (ch1) is highly opaque to atmospheric aerosols, obscuring most of the signal from dark vegetation and providing little useful information about burned areas. Red reflectance (ch2) initially decreases in relation to unburned forest due to strong absorption by ash, then gradually increases after ash is removed and there remains little chlorophyll absorption in red wavelengths relative to unburned forest (figure 1(*c*)). The NIR channel (ch3) shows the largest initial change, with reflectance dropping to less than 50% that of unburned forest. As previously observed with Landsat TM (White *et al.* 1996), NIR reflectance rapidly recovers after burning due to regrowth of herbaceous and other early successional vegetation.

The response of the SWIR band (ch4) is more difficult to interpret since it changes direction. Immediately following fire, the SWIR decreases owing to strong absorption by ash and char as is observed in burned African savannah (figure 1(*c*), Eva and Lambin 1998). As the signal from the combustion products becomes less prominent with vegetation regrowth and rainfall, the SWIR increases monotonically, eventually showing the largest difference relative to other VGT channels. During this period, SWIR reflectance of burned forest becomes comparatively larger because there is little vegetation water content, which strongly absorbs SWIR radiation in the surrounding, dense unburned forest (Chuvieco and Congalton 1988, White *et al.* 1996). An elevated SWIR signature and fire boundary can still be observed in many regenerating forests in Alberta and Saskatchewan that are shown in historical fire

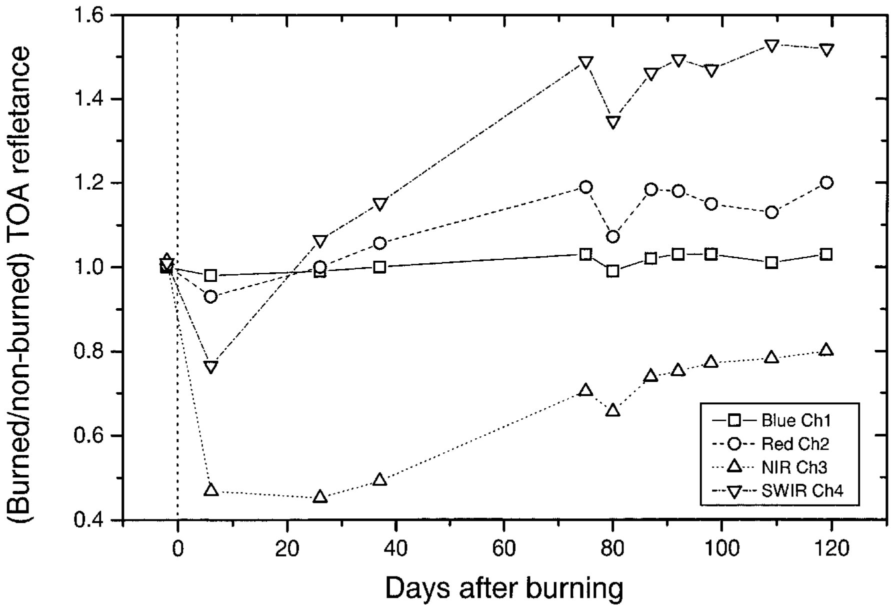

Figure 2. Temporal evolution of TOA reflectance from VEGETATION, shown using the ratio of burned reflectance (80 pixels) to non-burned reflectance (84 pixels). Data from the active fire images (5 May and 8 May) are not shown.

records to have burned in 1981, or 17 years previously. In addition, Eastwood *et al.* (1998) demonstrated that several year-old forest burns in Manitoba, Canada could be most effectively discriminated using VGT's SWIR channel, which was simulated using Landsat TM data.

The evolution of the NDVI, computed from TOA reflectances as (ch3–ch2/ ch3 + ch2), is shown in figure 3 for burned and unburned forest. As in the case of the NIR, NDVI provides maximal separation immediately following fire, which then gradually diminishes over time. Exploiting the large SWIR response to burning, a short-wave vegetation index (SWVI) can be formulated using (ch3 − ch4/ch3 + ch4). The index is analogous to VI3 for AVHRR (Kaufman and Remer 1994) and to indices proposed for Landsat TM (Garcia and Caselles 1991, Jurgens 1997). The relative SWVI difference between burned and non-burned forest is greater than that of NDVI except for the date immediately following the fire (figure 3). This is also illustrated in figure 4, which shows NDVI and SWVI images of the Swan Hills burn computed from the 3 August VGT scene. The larger difference can be attributed to the similar, but stronger SWIR response compared to the red channel after burning (figure 2). By replacing the red channel with SWIR, the SWVI has the added advantage of being less sensitive to smoke contamination, since the SWIR is relatively transparent to aerosols (Kaufman and Remer 1994). In general, the NIR/MIR bi-spectral domain has been found to be effective for discriminating a variety of burned vegetation types (Garcia and Caselles 1991, Kushla and Ripple 1998, Barbosa *et al.* 1999, Pereira 1999).

6. Conclusions

SPOT VGT imagery is highly effective for discriminating burned boreal forest, owing to the inclusion of a 1.65 μm SWIR channel that is sensitive to vegetation

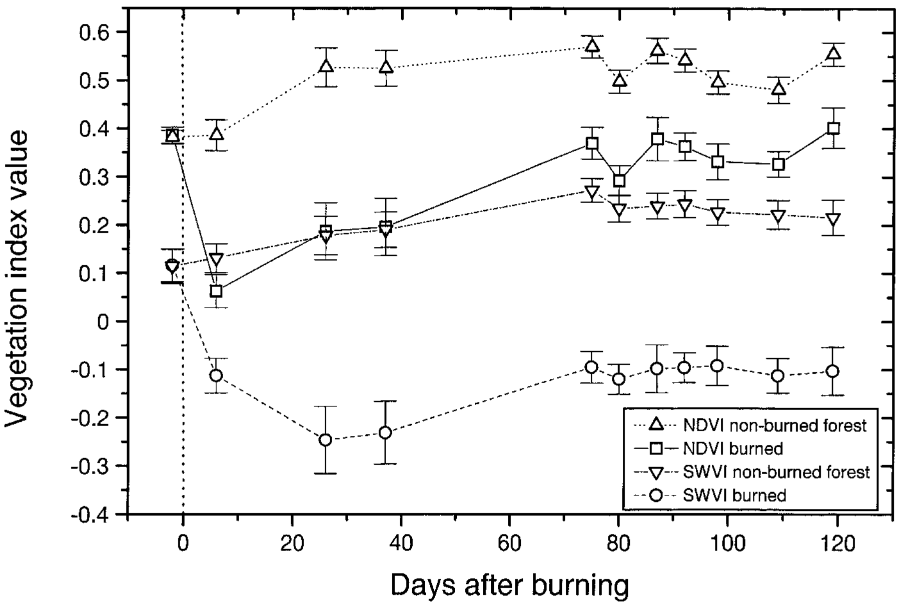

Figure 3. Temporal evolution of the Normalized Difference Vegetation Index (NDVI) and Short-wave Vegetation Index (SWVI) for burned forest (80 pixels) and non-burned forest (84 pixels). The error bars represent standard deviations. Data from the active fire images (5 May and 8 May) are not shown.

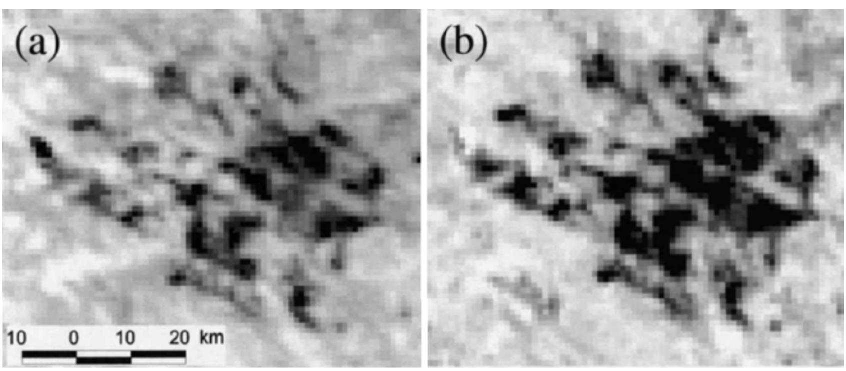

Figure 4. The Virginia Hills burn shown using (*a*) Normalized Difference Vegetation Index (NDVI) and (*b*) Short-wave Vegetation Index (SWVI), which were computed using a VEGETATION image from 3 August, 1998.

water content. The SWIR channel exhibits a strong and prolonged response to burning, generally lasting several years. A normalized vegetation index (SWVI) that combines the NIR and SWIR channels provides better separation of burned forest compared to NDVI or individual channels. Multi-temporal differencing of the SWVI from anniversary date 10-day composites is currently being synergistically combined with annual AVHRR hotspots (Fraser *et al.* 2000) to map forest that burned in Canada during 1998 and 1999. The SWIR channel also can be used to detect active boreal fires, although the 3.7 μm channel aboard AVHRR provided a significantly higher detection rate.

Acknowledgments

We thank Ji-zhong Jin at CCRS for assisting in processing the SPOT-4 VEGETATION imagery. The imagery and partial funding was provided through a VEGETATION Preparatory Program investigation led by Jing Chen at CCRS.

References

AHERN, F. J., and ARCHIBALD, P. D., 1986, Thematic Mapper information about Canadian forests: early results from across the country. *Proceedings of the Tenth Canadian Symposium on Remote Sensing*, 5–8 May 1986 (Ottawa: Canadian Aeronautics and Space Institute), pp. 683–697.

BARBOSA, P. M., GREGOIRE, J. M., and PEREIRA, J. M. C., 1999, An algorithm for extracting burned areas from time series of AVHRR GAC data applied at a continental scale. *Remote Sensing of Environment*, **69**, 253–263.

CAHOON, D. R., STOCKS, B. J., LEVINE, J. S., COFER, W. R., and PIERSON, J. M., 1994, Satellite analysis of the severe 1987 forest fires in northern China and southeastern Siberia. *Journal of Geophysical Research*, **99**, 18627–18638.

CANADIAN COUNCIL OF FOREST MINISTERS, 1999, National Forestry Database Program. Canadian Forest Service, Natural Resources Canada. http://nfdp.ccfm.org/

CHUVIECO, E., and CONGALTON, R. G., 1988, Mapping and inventory of forest fires from digital processing of TM data. *Geocarto International*, **4**, 41–53.

COFER, W. R., WINSTEAD, E. L., STOCKS, B. J., OVERBAY, L. W., GOLDAMMER, J. G., CAHOON, D. R., and LEVINE, J. S., 1996, Emissions from boreal forest fires: are the atmospheric impacts underestimated? In *Biomass Burning*, edited by J. S. Levine (Cambridge, MA: MIT Press), pp. 834–839.

EASTWOOD, J. A., PLUMMER, S. E., WYATT, B. K., and STOCKS, B. J., 1998, The potential of SPOT-Vegetation data for fire scar detection in boreal forests. *International Journal of Remote Sensing*, **19**, 3681–3687.

EVA, H., and LAMBIN, E. F., 1998, Burnt area mapping in Central Africa using ATSR data. *International Journal of Remote Sensing*, **19**, 3473–3497.

FLANNIGAN, M. D., and VONDER HAAR, T. H., 1986, Forest fire monitoring using NOAA satellite AVHRR. *Canadian Journal of Forestry Research*, **16**, 975–982.

FRASER, R. H., LI, Z., and CIHLAR, J., 2000, Hotspot and NDVI differencing synergy (HANDS): a new technique for burned area mapping over boreal forest. *Remote Sensing of Environment*, in press.

FRENCH, N. H., KASISCHKE, E. S., JOHNSON, R. D., BOURGEAU-CHAVEZ, L. L., FRICK, A. F., and USTIN, S., 1996, Estimating fire-related carbon flux in Alaskan boreal forests using multisensor remote-sensing data. In *Biomass Burning and Global Change*, edited by J. S. Levine (Cambridge, MA: MIT Press), pp. 808–826.

GARCIA, M. J., and CASELLES, V., 1991, Mapping burns and natural reforestation using thematic mapper data. *Geocarto International*, **1**, 31–37.

JURGENS, C., 1997, The modified normalized difference vegetation index (nNDVI)—a new index to determine frost damages in agriculture based on Landsat TM data. *International Journal of Remote Sensing*, **18**, 3583–3594.

KASISCHKE, E. S., and FRENCH, N. H., 1995, Locating and estimating the areal extent of wildfires in Alaskan boreal forests using multiple-season AVHRR NDVI composite data. *Remote Sensing of Environment*, **51**, 263–275.

KAUFMAN, Y. J., and REMER, L. A., 1994, Detection of forests using mid-IR reflectance: an application for aerosol studies. *IEEE Transactions on Geoscience and Remote Sensing*, **32**, 672–683.

KNEPPECK, I. D., and AHERN, F. J., 1989, Stratification of a regenerating burned forest in Alberta using Thematic Mapper and C-SAR images. *Proceedings of the International Geoscience and Remote Sensing Symposium* (IGARSS), 10–14 July 1989 (Ottawa: IGARSS '89 12th Canadian Symposium on Remote Sensing), pp. 1391–1396.

KUSHLA, J. D., and RIPPLE, W. J., 1998, Assessing wildfire effects with Landsat thematic mapper data. *International Journal of Remote Sensing*, **19**, 2493–2507.

LEVINE, J. S., COFER, W. R., CAHOON, D. R., and, WINSTEAD, E. L., 1995, Biomass burning: a driver for global change. *Environmental Science & Technology*, **29**, 120–125.

Li, Z., Nadon, S., and Cihlar, J., 2000a, Satellite mapping of Canadian boreal forest fires: evaluation and comparison of algorithms. *International Journal of Remote Sensing*, in press.

Li, Z., Nadon, S., Stocks, B., and Cihlar, J., 2000b, Satellite detection of Canadian boreal forest fires: development and application of the algorithm. *International Journal of Remote Sensing*, in press.

Pereira, J. M. C., 1999, A comparative evaluation of NOAA/AVHRR vegetation indexes for burned surface detection and mapping. *IEEE Transactions on Geoscience and Remote Sensing*, **37**, 217–226.

Rauste, Y., Herland, E., Frelander, H., Soini, K., Kuoremaki, T., and Ruokari, A., 1997, Satellite-based forest fire detection for fire control in boreal forests. *International Journal of Remote Sensing*, **18**, 2641–2656.

Stocks, B. J., 1991, The extent and impact of forest fires in northern circumpolar countries. In *Global Biomass Burning: Atmospheric, Climatic, and Biospheric Implications*, edited by J. S. Levine (Cambridge, MA: MIT Press), pp. 197–202.

White, J. D., Ryan, K. C., Key, C. C., and Running, S. W., 1996, Remote sensing of forest fire severity and vegetation recovery. *International Journal of Wildland Fire*, **66**, 125–136.